# Studies on the Iron(II) *meso*-Oxyporphyrin $\pi$-Neutral Radical as a Reaction Intermediate in Heme Catabolism

**Isao Morishima,* Hiroshi Fujii,† and Yoshitsugu Shiro‡**

Division of Molecular Engineering, Graduate School of Engineering, Kyoto University, Kyoto 606, Japan

**Seiyo Sano§**

Department of Public Health, Faculty of Medicine, Kyoto University, Kyoto 606, Japan

*Received July 12, 1994*⊗

The electronic structure of iron(III) *meso*-hydroxyporphyrin (**2a**) dissolved in pyridine was characterized by NMR, ESR, and optical absorption spectroscopies. It was found that the *meso* hydroxyl group of **2a** is fully deprotonated in pyridine solution, and the resultant compound is in a quantum mixing state of the iron(III) *meso*-oxyporphyrin (**2b**) and the iron(II) porphyrin $\pi$-neutral radical (**2c**) states, i.e., the resonance structure of **2b** and **2c**. Deprotonation of the *meso* hydroxyl group and coordination of the axial ligands are both essential for the generation of this unique electronic structure. The population of **2b** and **2c** in the mixing state is modulated by the basicity of the axial ligands, as was manifested by the drastic NMR and ESR spectral changes upon varying the pyridine derivatives as the ligands. Because **2c** is highly reactive with $O_2$ to form verdoheme, while **2a** and **2b** are unreactive, the formation of the $\pi$-radical character is essential in heme breakdown. Thus, we discussed the electronic structure of *meso*-hydroxyheme in relation to the reaction of heme catabolism.

## Introduction

In a biological system, the endogenous heme in hemoglobin and myoglobin is degraded to a bile pigment by catalysis with an enzyme, heme oxygenase, which is localized in a microsomal fraction obtained from the spleen, bone marrow, and liver.[1] The heme oxygenase requires 3 mol of $O_2$ and NADPH[1] and cleaves the *meso* α-position of the iron protoporphyrin IX complex to produce biliverdin Xα and CO.[2] With relevance to the biological heme degradation reaction,[3] Lemberg and colleagues studied the chemical heme cleavage reaction, viz. coupled oxidation (Scheme 1); treatment of bis(pyridine)iron(II) porphyrin with hydrogen peroxide or of bis(pyridine)iron(III) porphyrin with oxygen and ascorbic acid in aqueous pyridine yields CO and verdohemochrome, followed by formation of biliverdin by sequential treatment with a base and an acid.[4]

The enzymatic and chemical reactions of the heme degradation are very unique, because they permit the stable prophyrin ring to be easily opened under extremely mild conditions.[5−7] Thus, a key intermediate which is very reactive with $O_2$ has been imagined to be involved in the heme degradation reaction. The characteristic visible spectrum ($\lambda_{max}$ = 639 nm) which was then observed in the coupled oxidation was believed to come from the intermediate in the heme degradation reaction.[8] This compound was initially thought to be a heme−peroxide complex but is now considered to be an iron(III) *meso*-hydroxyporphyrin (**2a** in Scheme 1).[9] On the other hand, Jackson et al. using a tritiated derivative have demonstrated that **2a** injected in rats is readily converted to the bile pigment.[10,11] Further, recent work by Sano and co-workers provided direct evidence for the oxidative cleavage of **2a** by $O_2$ using chemically synthesized iron(III) α-*meso*-hydroxyprotoporphyrin.[12] On the basis of these comprehensive studies, it is now convincing that **2a** is the key intermediate in heme degradation.

A number of studies have been carried out to characterize the electronic structure of *meso*-hydroxyporphyrin. Bonnett[13] and Fuhrhop and co-workers[14] comprehensively studied the electronic structures and reactivities of some metal complexes of *meso*-hydroxyporphyrin or oxophlorin in relation to the porphyrin degradation reaction. Recently, Balch et al. characterized the structure of metal (Mn, Co, Ni) complexes of *meso*-oxyoctaethylporphyrin.[15] They showed that the porphyrin ligand is either twisted into ruffled shapes or lies in a plane, depending

* To whom correspondence should be addressed. Fax: +81-75-751-7611.
† Present address; Institute for Life Support Technology, Yamagata Technopolis Foundation, Kurumanomae 683, Numagi, Yamagata 990, Japan.
‡ Present address: Institute of Physical and Chemical Research (RIKEN), Wako 351-01, Japan.
§ Present address: Shiga University of Medical Science, Otsu 520-21, Japan.
⊗ Abstract published in *Advance ACS Abstracts,* February 15, 1995.

(1) (a) Tenhunen, R.; Marver, H. S.; Schmid, R. *Proc. Natl. Acad. Sci. U.S.A.* **1968**, *61*, 748−755. (b) Tenhunen, R.; Marver, H. S.; Schmid, R. *J. Biol. Chem.* **1969**, *244*, 6388−6894. (c) Tenhunen, R.; Marver, H. S.; Schmid, R. *J. Lab. Chem.* **1970**, *75*, 410−421.
(2) Tenhunen, R.; Marver, H. S.; Pimstone, N. R.; Trager, W. F.; Cooper, D. Y.; Schmid, R. *Biochemistry* **1972**, *11*, 1716−1720.
(3) (a) Yoshida, T.; Kikuchi, G. *J. Biol. Chem.* **1978**, *253*, 4224−4229. (b) Yoshida, T.; Kikuchi, G. *J. Biol. Chem.* **1978**, *253*, 4230−4236.
(4) Lemberg, R. *Biochem. J.* **1935**, *29*, 1322−1335.
(5) Clezy, P. S.; Liepa, A. J. *Aust. J. Chem.* **1970**, *23*, 2477.
(6) Jackson, A. H.; Kenner, F. W.; Smith, K. M. *J. Chem. Soc. C* **1968**, 302−310.
(7) (a) Bonnett, R.; Dimsdale, M. J. *J. Chem. Soc., Perkin Trans. 1* **1972**, 2540−2548. (b) Bonnett, R.; Dimsdale, M. J.; Stephenson, G. F. *J. Chem. Soc. C* **1969**, 564−570.
(8) Lemberg, R.; Cortis-Jones, B.; Norrie, M. *Nature* **1937**, *139*, 1016−1017.
(9) (a) Lemberg, R.; Cortis-Jones, B.; Norrie, M. *Biochem. J.* **1938**, *32*, 171−186. (b) Bonnett, R.; McDonagh, A. F. *J. Chem. Soc., Chem. Commun.* **1970**, 237−238.
(10) Jackson, A. H.; Kenner, F. W.; McGillivrav, G.; Smith, K. M. *J. Chem. Soc. C* **1968**, 294−302.
(11) Kondo, T.; Nicholson, D. C.; Jackson, A. H.; Kenner, G. W. *Biochem. J.* **1971**, *121*, 601−607.
(12) Sano, S.; Sano, T.; Morishima, I.; Shiro, Y.; Maeda, Y. *Proc. Natl. Acad. Sci. U.S.A.* **1986**, *83*, 531−535.
(13) Bonnett, R.; Dimsdale, M. J.; Sales, K. D. *J. Chem. Soc. Chem. Commun.* **1970**, 962−963.
(14) Fuhrhop, J.-H.; Besecke, S.; Subramanian, J.; Mengersen, Chr.; Riesner, D. *J. Am. Chem. Soc.* **1975**, *97*, 7141−7152.

0020-1669/95/1334-1528$09.00/0 

**Scheme 1**

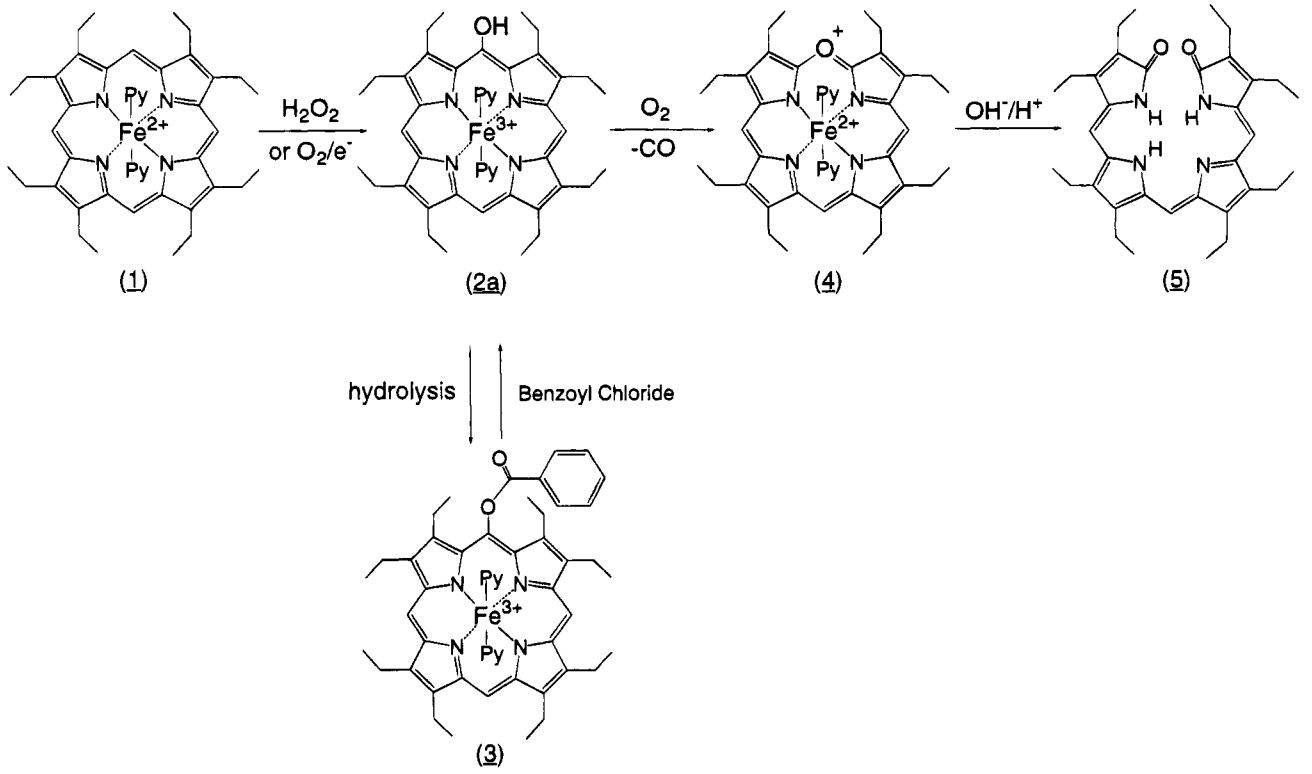


on the metal and its coordination. However, concerning the iron complex of *meso*-hydroxyporphyrin, the electronic structure was not experimentally identified, until we observed its unusual hyperfine-shifted proton NMR spectrum in pyridine.[12,16] We explained its uniquely large hyperfine shifts of *meso* protons in terms of a porphyrin $\pi$-radical character rather than an iron(III) state, by comparing the NMR spectrum with those for metalloporphyrin $\pi$-cation radicals.[17] In combination with the Mössbauer results,[12] we concluded that **2a** in pyridine is in an iron(II) *meso*-oxyporphyrin $\pi$-neutral radical or an oxophlorin radical state (**2c**).

In the present study, we further examined the mechanism of formation of the iron(II) oxoporphyrin $\pi$-neutral radical from **2a** in pyridine and characterized its electronic structure in more detail by analyzing the axial ligand effect on NMR, ESR, and optical spectral features of **2a**. Their unique spectral features can be reasonably and consistently explained in terms of the resonance state of iron(III) *meso*-oxyporphyrin (**2h**) and the iron(II) *meso*-oxyporphyrin $\pi$-neutral radical (**2c**). We also discussed the electronic structure in relation to the reactivity of the compound toward $O_2$ under various conditions. Our present comprehensive work will provide a clue to unveil the reaction mechanism of heme breakdown in the heme oxygenase system.

## Experimental Section

**Materials.** Pyridine was distilled over sodium hydroxide. 4-Acetylpyridine, 4-methylpyridine, 3,4-dimethylpyridine, and 1-methylimidazole were purchased from Wako and were distilled under reduced pressure before use. Pyridine-$d_5$ was purchased from Merck and used without further purification. Octaethylporphyrin (OEP) was prepared by the method of Inhoffen et al.[18]

**Spectral Measurements.** Absorption spectral measurements were made on a Hitachi 330 spectrometer. Low-temperature absorption spectra were obtained using a DN 1704 variable-temperature liquid-nitrogen cryostat (Oxford Instruments). Proton NMR spectra of 300 MHz and deuterium NMR spectra at 46.1 MHz were recorded with a Nicolet NT-300 spectrometer equipped with a 1280 computer system. The $^1$H-NMR spectrum of **2a** in pyridine was measured in a neat pyridine-$d_5$. When 4-acetylpyridine, 4-methylpyridine, 3,4-dimethylpyridine, or 1-methylimidazole was used as an $^1$H-NMR solvent, a conventional solvent-eliminating Fourier transform pulse sequence (180°−$\tau$−90°−acquire) was employed to minimize the solvent signals. NMR signals of **2a** in various solvents were assigned by *meso*-deuterium-labeled compound signal intensity and variable-temperature measurements. ESR spectra were recorded at 77 K with a JEOL JES-3X spectrometer operating with 100-kHz magnetic field modulation.

**Chloroiron(III) *meso*-(Benzoyloxy)octaethylporphyrin (3).** *meso*-(Benzoyloxy)porphyrin was prepared by the method of Bonnett et al.[7] Incorporation of iron into the porphyrin was accomplished by addition of ferrous chloride and sodium acetate to a refluxing solution of the porphyrin in acetic acid under an argon atmosphere and subsequent stirring for 2 h. After the mixture was cooled to room temperature, the precipitate was collected by filtration and washed by water. UV−vis ($CH_2Cl_2$), nm (relative intensity): 385 (1.000), 507 (0.092), 537 (0.065), 583 (0.026), 638 (0.041). $^1$-NMR ($CD_2Cl_2$; 23 °C), ppm: 45.8, 45.2, 43.9 (2H), 43.2, 42.6 (2H), 41.3 (2H), 40.8 (2H), 399.2, 36.7, 36.2 (2H) (methylene proton) and −56.2, −62.4, −65.8, −70.2 (*meso* proton).

**Chloroiron(III) *meso*-hydroxyoctaethylporphyrin-*meso*-$d_3$** was synthesized using octaethylporphyrin-*meso*-$d_4$, which was made by sulfuric acid-$d_2$ exchange.[19]

**Iron(III) *meso*-Hydroxyoctaethylporphyrin (2a).** Chloroiron(III) *meso*-(benzoyloxy)octaethyl porphyrin was dissolved in methanol, and the solution was degassed for 1 h. Sodium hydroxide in methanol was

(15) (a) Balch, A. L.; Noll, B. C.; Reid, S. M.; Zovinka, E. P. *J. Am. Chem. Soc.* **1993**, *115*, 2531−2532. (b) Balch, A. L.; Noll, B. C.; Reid, S. M.; Zovinka, E. P. *Inorg. Chem.* **1993**, *32*, 2610−2611. (c) Balch, A. L.; Noll, B. C.; Phillips, S. L.; Reid, S. M.; Zovinka, E. P. *Inorg. Chem.* **1993**, *23*, 4730−4736.
(16) Morishima, I.; Fujii, H.; Shiro, Y.; Sano, S. *J. Am. Chem. Soc.* **1986**, *108*, 3858−3860.
(17) (a) Morishima, I.; Shiro, Y.; Takamuki, Y. *J. Am. Chem. Soc.* **1983**, *105*, 6168−6170. (b) Morishima, I.; Takamuki, Y.; Shiro, Y. *J. Am. Chem. Soc.* **1984**, *106*, 7666−7672. (c) Morishima, I.; Shiro, Y.; Nakajima, K. *Biochemistry* **1986**, *25*, 3576−3584.
(18) Inhoffen, H. H.; Fuhrhop, J. H.; Brockmann, H. V. H., Jr. *Ann. Chem.* **1966**, *695*, 133−143.
(19) Bonnett, B.; Gale, I. A. P.; Stephenson, G. F. *J. Chem. Soc. C* **1967**, 1168−1172.

added slowly to the refluxing solution under argon atmosphere. The mixture was refluxed for 2 h. After cooling to room temperature, the mixture was poured into water, and the iron complex was extracted with chloroform. The chloroform solution was washed with dilute HCl and water. After evaporation of the solvent, the residual microcrystalline solid was dried under vacuum. UV−vis ($CHCl_3$), nm: 390, 490 (sh), 520 (sh), 690. $^1$H-NMR ($CDCl_3$; 23 °C), ppm: 39.4, 37.0, 34.1, 31.8, 30.0, 28.7, 23.0, 18.1 (methylene proton), −28.1, −100.0 (*meso* proton).

**Preparation of Samples.** All preparations of samples for spectral measurements were carried out using a specially designed Thunberg-type vessel[12] connected to a vacuum line. Pyridine solution was degassed by the freez−pump−thaw method three times. **2a** was added to the Thunberg vessel, and the vessel was evacuated. The degassed pyridine was transferred into the Thunberg vessel by vacuum distillation. After the vessel was sealed, **2a** was dissolved in the pyridine. **2a** in pyridine was transferred into a cell (UV−vis or NMR), and the cell was sealed under vacuum conditions.

## Results and Discussion

**Formation of Iron(II) *meso*-Oxyporphyrin $\pi$-Neutral Radical in Pyridine.** Iron(III) *meso*-hydroxyoctaethylporphyrin dissolved in pure pyridine under anaerobic conditions displayed a very characteristic $^1$H-NMR spectrum (Figure 1a), where two well-resolved proton resonances with two and one proton intensities were observed at −111 and −154 ppm, respectively. These signals can be assigned to the porphyrin *meso* protons by utilizing the $^2$H-NMR signals of the *meso*-deuterium-labeled compound. Four methylene proton signals were uniquely observed at 31.6, 4.5, 2.1, and −2.5 ppm, and four methyl proton signals were located in the region 2.3−3.4 ppm.

In this NMR spectrum, the most remarkable finding is the far upfield shift of the *meso* proton resonances. The magnetic susceptibility of this compound measured by the NMR Evans method is $\mu_{eff} = 2.4\ \mu_B$ at 296 K, suggesting that the unique hyperfine-shifted NMR spectrum arises from the paramagnetism of a single electron spin ($S = {}^1/_2$). However, this spectral feature has been unprecedented for the metal-centered paramagnetic iron porphyrin compounds reported so far. Indeed, the *meso* proton resonances of the imidazole complex of ferric **3** (7 and 0.6 ppm) did not exhibit such a far upfield shift as those found for **2a** in pyridine. Further, Mössbauer measurements of **2a** in pyridine at 77 K gave values of $\Delta E_q = 1.3$ mm/s and $\delta = 0.2$ mm/s, which are also different from those of bis(pyridine)iron(III) porphyrin compounds.[20] Rather, the signal positions of the *meso* protons are very similar to those of the metalloporphyrin $\pi$-radicals reported so far. Therefore, it can be suggested that the unpaired spin density delocalized on the porphyrin $\pi$ system, i.e. the $\pi$-radical character, predominantly contributes to the characteristic hyperfine shifts of the *meso* proton signals for **2a** in pyridine.

It is very interesting to examine the mechanism of the generation of the $\pi$-radical character from **2a** in pyridine. We previously reported that, upon titration with diluted HCl, the optical absorption spectrum of **2a** in pyridine with four isosbestic points became a spectrum similar to that of a ferric low-spin porphyrin compound, such as the bis(imidazole) complex of **3**.[16] We followed the same reaction of **2a** by $^1$H-NMR spectroscopy, as illustrated in Figure 1. Upon addition of acid to the pyridine solution of **2a**, the far upfield shifted *meso*-proton resonances (in Figure 1a) moved downfield, and the resultant spectrum (Figure 1d) was similar to that of the bis(imidazole) complex of **3** consistent with the visible absorption spectral results.

The observed NMR spectral change showed that protonation of the compound causes the $\pi$-radical character to decrease. In other words, deprotonation of **2a** generates the $\pi$-radical character. Because **2a** possesses a phenolic character, the *meso* hydroxyl group of this compound is readily deprotonated in pyridine to form the enolate anion (**2b**). Thus, one possible mechanism for formation of the porphyrin $\pi$-radical character without a reducing reagent is an intramolecular electron transfer from the enolate anion of the porphyrin to the central iron, yielding the iron(II) *meso*-oxyporphyrin $\pi$-neutral radical (**2c**). The electronic structure of this compound will be studied in more detail in the next section.

**Effect of Axial Ligand Basicity on the Electronic State of the *meso*-Oxyporphyrin $\pi$-Neutral Radical.** The **2a** compound in pyridine is very reactive with $O_2$, yielding verdohemochrome (**4**), which is a precursor of biliverdine (**5**) and bilirubin, which is suggestive of the importance of the $\pi$-radical character for the reactivity of **2a** with $O_2$. Indeed, the same reaction does not occur in $CH_2Cl_2$. The proton of the *meso* hydroxyl group in **2a** must dissociate in the basic solution for the $\pi$-radical formation. However, it is worthwhile to mention that **2a** is unreactive with $O_2$ in an aqueous alkaline solution, in which the *meso* hydroxyl group is fully deprotonated. Furthermore, we also observed that the $\pi$-radical was not generated from **2a** in 2,6-di-*tert*-butylpyridine, which is a base but which cannot coordinate to the iron as an axial ligand. These observations suggested that coordination of the ligand to the iron as well as the deprotonation of the *meso* hydroxyl group are probably both essential for the formation of the $\pi$-radical character and eventually for the high reactivity with $O_2$.

Thus, in order to gain further insight into the formation of the $\pi$-radical character from **2a** and into its detailed electronic structure, we examined the axial ligand effect with $^1$H-NMR, ESR, and optical absorption spectroscopies. We chose various solvents (ligands) having a variety of basicities as follows: 4-acetylpyridine (Acpy, $pK_a = 3.51$), pyridine (py, $pK_a = 5.28$), 4-methylpyridine (Mepy, $pK_a = 5.98$), 3,4-dimethylpyridine (diMepy, $pK_a = 6.46$), and 1-methylimidazole (MeIm, $pK_a = 7.20$).[21] We dissolved **2a** in each solvent under anaerobic conditions and measured the spectra. These pyridine and imidazole derivatives can serve as both bases and axial ligands for iron.

In the $^1$H-NMR spectra of **2a** (Figure 2), the methylene and the *meso* proton signals characteristically change in their position depending on the solvent (ligand) properties. In particular, the signal position of the *meso* proton, which serves as a sensitive indicator of the $\pi$-radical character, is affected by the solvent (ligand) basicity; e.g. the signals in Acpy are observed at −142 and −196 ppm, while those in MeIm are located at −40 ppm. With an increase in the solvent (ligand) $pK_a$ value, the signals dramatically move downfield, accompanied by signal sharpening.

Figure 3 shows the ESR spectra of **2a** at 77 K in various solvents. The ligand effects are observed in the $g$ values and the signal shape. An extreme case, **2a** in Acpy, exhibits an axial type spectrum, in which the signals are observed at $g =$ 2.2 and 1.9. With an increase in the solvent (ligand) basicity, the signal in the low field shifts further downfield, while the high-field signal moves higher. Finally, three absorptions are resolved at $g = 2.53$, 2.28, and 1.66 for the MeIm complex, which closely resemble those for the ferric imidazole complex of **3** (Figure 3f). All of these NMR and ESR results are assembled in Table 1.

(20) Epstein, L. M.; Straub, D. K.; Maricondi, C. *Inorg. Chem.* **1967**, *6*, 1720−1724.

(21) Schoefield, K. In *Hetero-aromatic Nitrogen Compounds*; Plenum Press: New York, 1967; p 146.

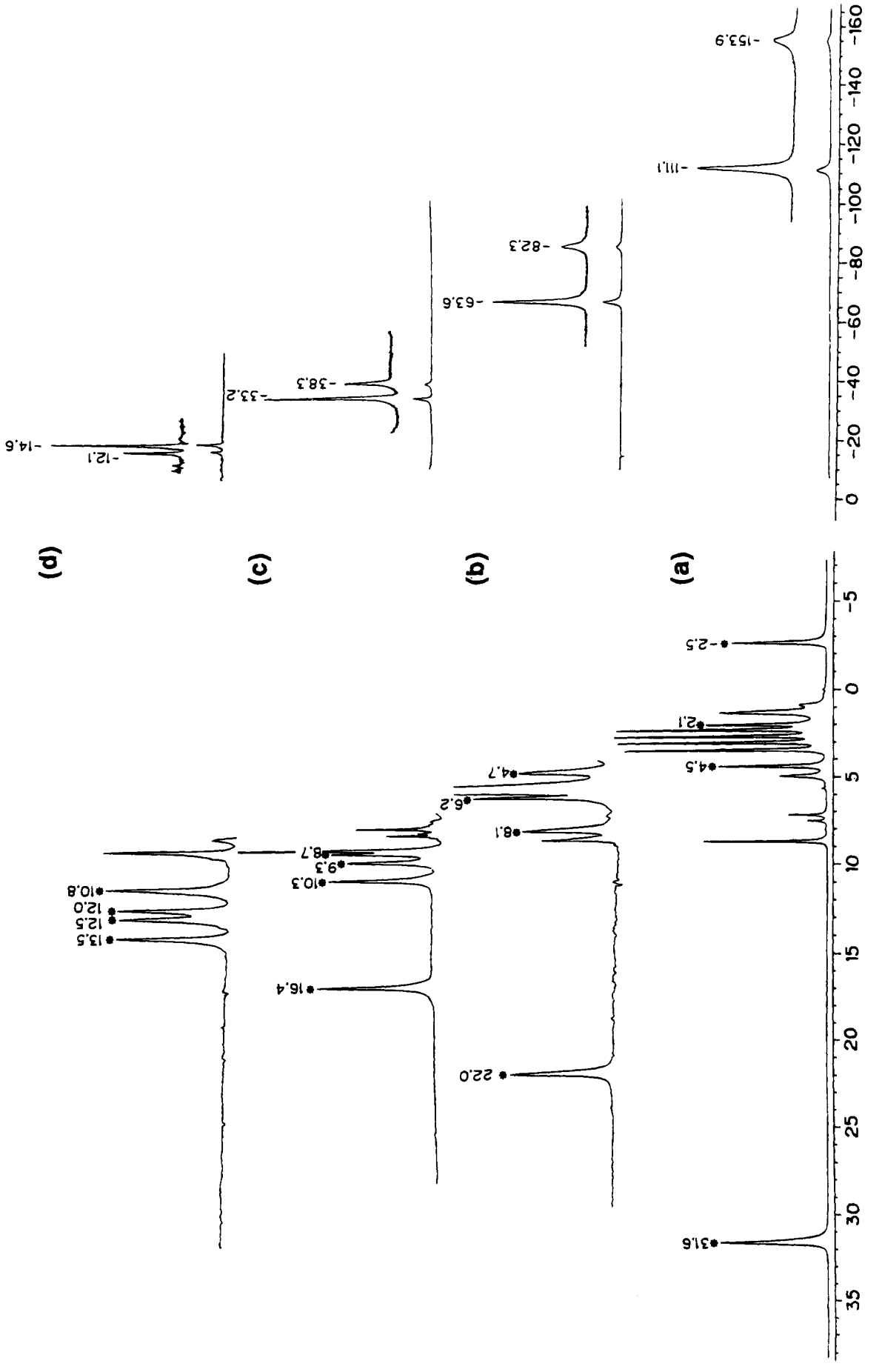


**Figure 1.** Proton NMR spectral changes of **2** in pyridine upon titration of methanol + HCl: (a) in pure pyridine-$d_5$; (b) in 300 $\mu$L of pyridine-$d_5$ and methanol (7:3) plus 3 $\mu$L of HCl (20%); (c) in 300 $\mu$L of pyridine-$d_5$ and methanol (1:1) plus 10 $\mu$L of HCl (20%); (d) in 300 $\mu$L of pyridine-$d_5$ and methanol (3:7) plus 30 $\mu$L of HCl (20%). When $CD_3OD$ and DCl are used instead of $CH_3OH$ and HCl, the *meso* 15-proton resonance disappears, due to H−D exchange. This was also the case for the iron-free oxophlorin radical and aminophlorin radical.

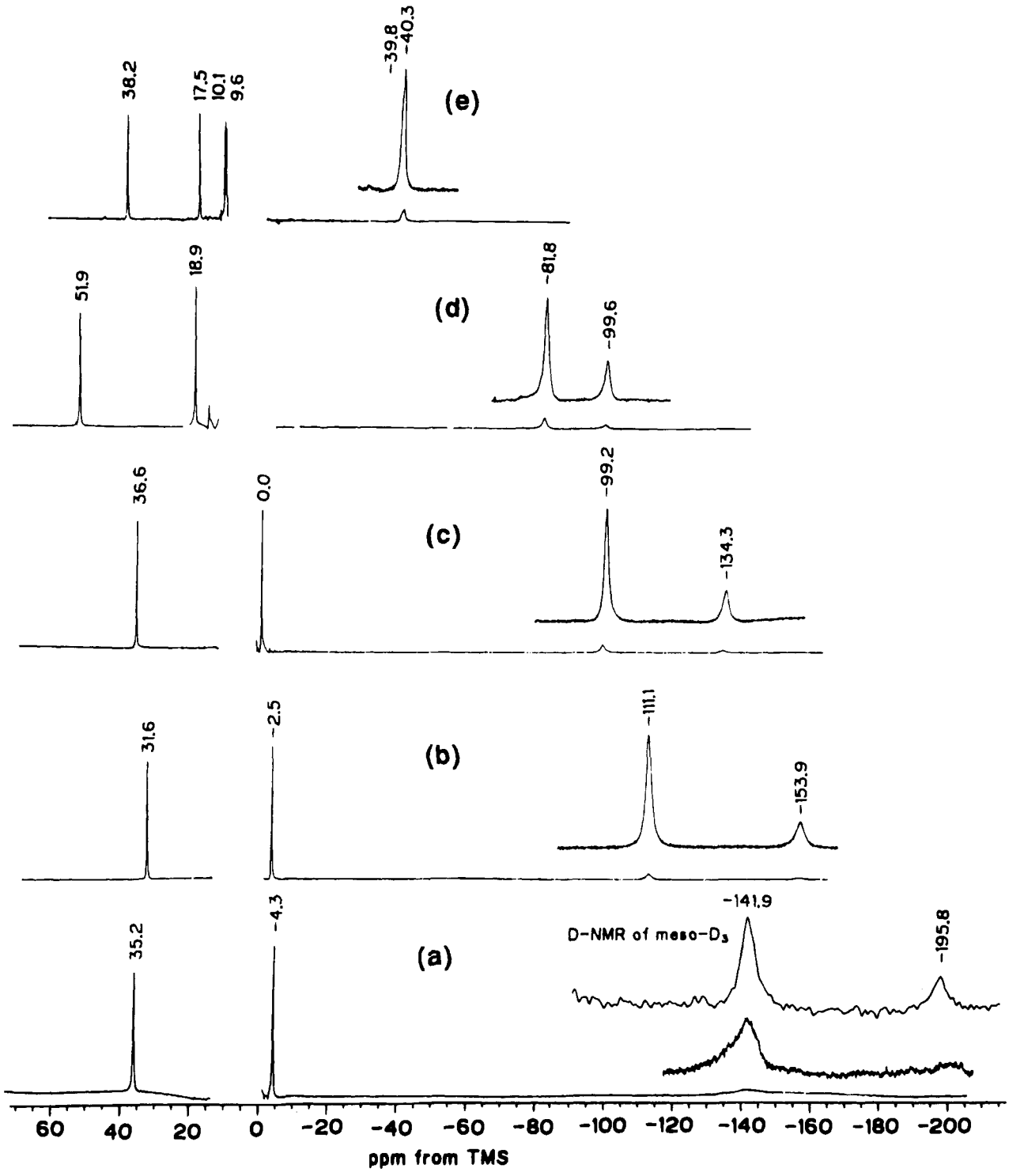


**Figure 2.** Proton NMR spectra of **2c** derivatives in neat pyridine and imidazole derivatives. **2** in pyridine was measured by using pyridine-$d_5$. Other pyridine derivatives and 1-methylimidazole were used in protonated solvents, so the signals in diamagnetic regions could not be observed: (a) in 4-acetylpyridine; (b) in pyridine; (c) in 4-methylpyridine; (d) in 3,4-dimethylpyridine; (e) in 1-methylimidazole.

In Figure 4 are illustrated their optical absorption spectra. With increasing solvent (ligand) p$K_a$ value, the absorption bands around 600 and 640 nm show a slight red shift and change in their relative intensities, and the Soret band also exhibits a blue shift. However, their characteristics are basically identical among the **2a** complexes with various ligands. Here, we also note that the spectral change is different from that of the acid titration experiment for **2a** in pyridine. All of these results thus suggest that the *meso* hydroxyl group in **2a** is in fully deprotonated form in all solvents employed, so that the NMR and ESR spectral features reflect the axial ligand effect on the electronic structure of the deprotonated form of **2a** (**2b**) and/or the $\pi$-neutral radical (**2c**) (see Scheme 2).

On the basis of the NMR signal position of the *meso* protons (Figure 2), with increasing ligand basicity, the $\pi$-radical character (**2c**) is decreased, with a concomitant increase in the Fe(III) character (**2b**). Our present results can thus be comparable to the mixing of the redox isomers of nickel porphyrin, where the Ni(II) porphyrin $\pi$-cation radical and Ni(I) porphyrin are admixed.[22] However, in the case of nickel porphyrin, the

(22) Mannassen, A.; Wolberg, A. *Inorg. Chem.* **1970**, *9*, 2365–2367.

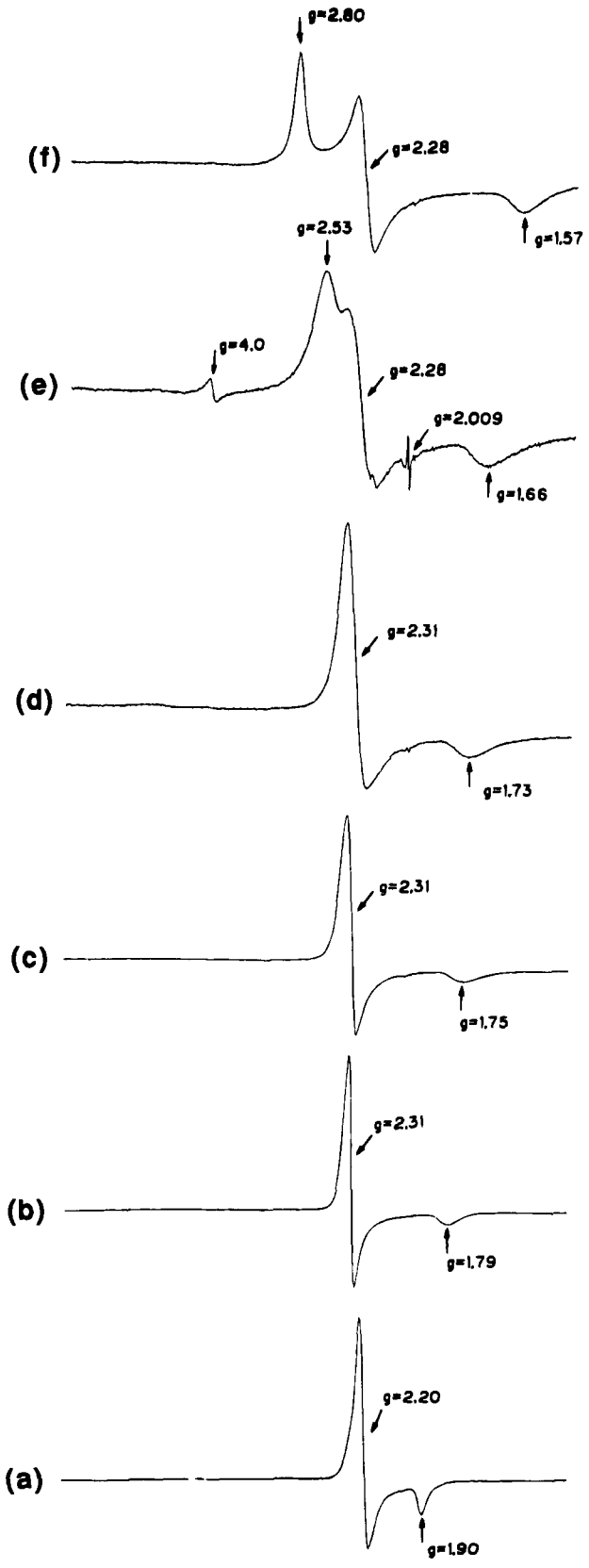


**Figure 3.** ESR spectra of **2c** derivatives in pyridine and imidazole derivatives and iron(III) *meso*-benzoyloxyoctaethylporphyrin bis(imidazole) at 77 K: (a) in 4-acetylpyridine; (b) in pyridine; (c) in 4-methylpyridine; (d) in 3,4-dimethylpyridine; (e) in 1-methylimidazole. Spectrum f is for **3a** in dichloromethane and excess imidazole.

ESR signals of these two states were separately observed, in sharp contrast with the present ESR features of **2a** (see Figure 3). We can then reasonably interpret the NMR, ESR, and

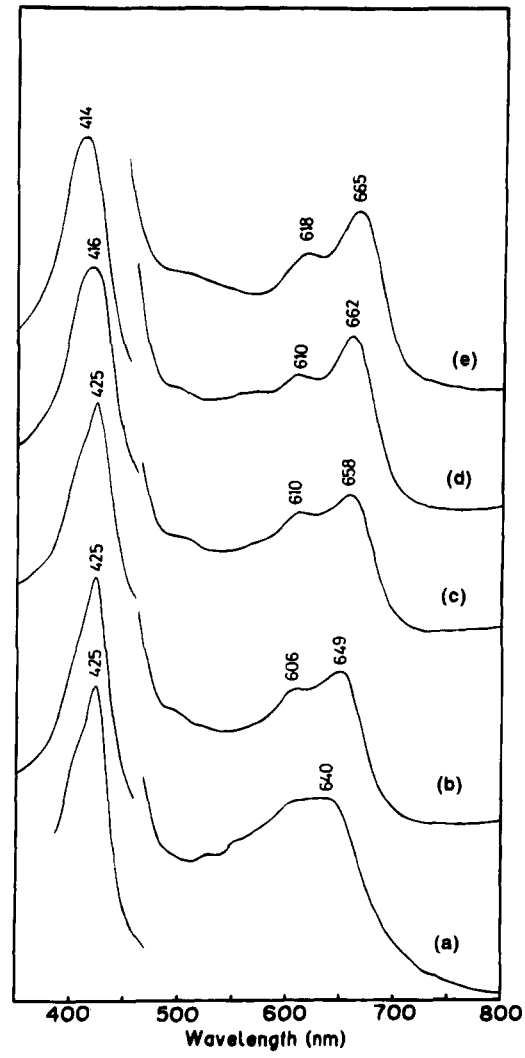


**Figure 4.** Absorption spectra of **2c** derivatives in neat pyridine and imidazole derivatives: (a) in 4-acetylpyridine; (b) in pyridine; (c) in 4-methylpyridine; (d) in 3,4-dimethylpyridine; (e) in 1-methylimidazole.

optical absorption spectral results for **2a** in terms of the resonance structure between **2b** and **2c** and the modulation of their relative contents by the ligand basicity. Namely, in the Acpy complex, the $\pi$-radical character (**2c**) is predominant, resulting in the far upfield shift of the *meso* proton NMR signals and the axial symmetric ESR spectrum. In contrast, the metal-centered paramagnetism ($Fe^{3+}$) in the MeIm complex, **2b**, mainly governs its $^1$H-NMR and ESR spectral features, which are quite similar to the corresponding ones of the ferric porphyrin compound. In general, strong ligands bound to the iron, i.e., ligands having high p$K_a$ values, stabilize the Fe(III) state more than the Fe(II) state, because of the low redox potential of the complex. On the other hand, the reduced state, Fe(II), is more stable in the iron porphyrin complex with weak axial ligands. If the redox potential of the *meso*-oxyprophyrin is comparable to that of the central iron, it seems reasonable that the iron in **2b** is readily reduced to generate **2c** by intramolecular electron transfer from the porphyrin moiety.

The electron transfer between the central metal and the porphyrin ring has been reported for Ni, Ru, Fe, and some other metal porphyrin complexes.[23-25] In these cases, where the porphyrin has $D_{4h}$ molecular symmetry, the porphyrin HOMO

(23) (a) Dolphin, D.; Niem, T.; Felton, R. H.; Fujita, I. *J. Am. Chem. Soc.* **1975**, *97*, 5288-5290. (b) Chang, D.; Malinski, T.; Ulman, A.; Kadish, K. M. *Inorg. Chem.* **1984**, *23*, 817-824.

**Table 1.** Spectral Characteristics of Iron(III) *meso*-Oxyoctaethylporphyrin

| complex | ligand | $^1$H-NMR (ppm) methylene | | | | *meso* | ESR | | | UV−vis (nm) | |
|---|---|---|---|---|---|---|---|---|---|---|---|
| **2c** | 4-acetylpyridine | 35.2<br>−195.8 | *a* | *a* | −4.3 | −141.9 | | 2.20 | 1.90 | 425 | 640 |
| | pyridine | 31.6<br>−153.9 | 4.5 | 2.1 | −2.5 | −111.1 | | 2.31 | 1.79 | 425 | 649 |
| | 4-methylpyridine | 36.6<br>−134.3 | *a* | *a* | 0.0 | −99.2 | | 2.31 | 1.75 | 425 | 658 |
| | 3,4-dimethylpyridine | 51.9<br>−99.9 | 18.9 | *a* | *a* | −81.8 | | 2.31 | 1.73 | 416 | 662 |
| | 1-methylimidazole | 38.2 | 17.5 | 10.1 | 9.6 | −40.3<br>−39.8 | 2.53 | 2.28 | 1.66 | 414 | 665 |
| (OEP)Fe$^{III}$ | imidazole | 6.2 | | | | 3.1 | 2.80 | 2.28 | 1.57 | 404 | 522 |

[a] Signal cannot be observed by overlapping of the solvent signals.

**Scheme 2**

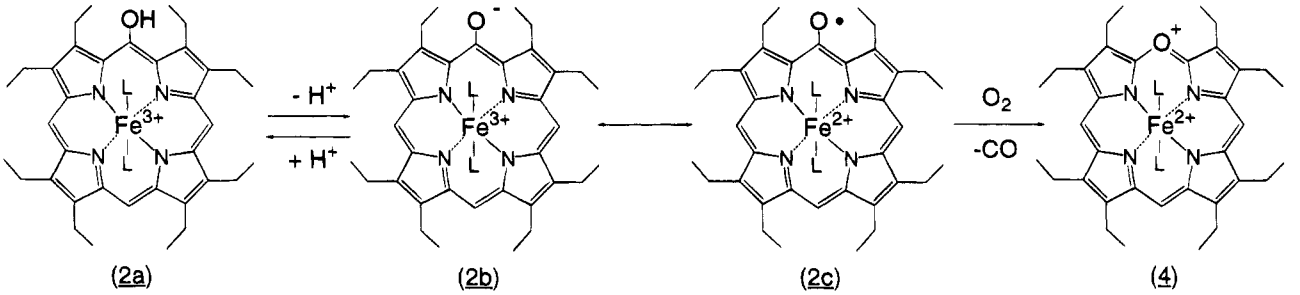


$\pi$ orbital cannot mix with the metal d$\pi$ orbitals. Therefore, the electron transfer for these complexes may presumably occur via the axial ligand or the counteranion. However, this is not the case for **2a**. Because of the $C_{2v}$ symmetry of the compound, the porphyrin HOMO, the $b_2$ orbital, is allowed to mix to some extent with the iron d$\pi$ orbital, which is favorable for the electron delocalization between the metal and the porphyrin ring. This is possibly the main reason for the resonance structure of **2b** and **2c** rather than the mixing of the two redox isomers.

In a previous report, we described the ESR spectrum of **2c** in pyridine as being quite similar to that of iron(I) tetraphenylporphyrin[26] and proposed that cooling of **2c** in pyridine to 77 K caused one more electron to be transferred from the porphyrin moiety to the iron(II) to generate the iron(I) compound.[27] However, when we measured the optical absorption spectrum of **2c** in pyridine at 77 K (data not shown), the spectrum was the same as that at room temperature (Figure 4), indicating no formation of the Fe(I) compound. The unique feature of the ESR spectra of **2a** in pyridine derivatives (Figure 3) could be reasonably explained in terms of the resonance structure of **2b** and **2c**: the quantum mixing of the ESR signal in a free radical type with that in a large $g_{max}$ type, which is characteristic of the bis(pyridine) complex of iron(III) porphyrin.[28] Mössbauer parameters also support the resonance structure of **2b** and **2c** but are inconsistent with those of iron(I) porphyrin and bis(pyridine)iron(III) porphyrin compounds.

**Biological Implications of the Electronic Structure of *meso*-Oxyporphyrin.** In the present study, we unambiguously describe the unique electronic structure of **2a** in pyridine, the resonance structure of **2b** and **2c**. This uniqueness is likely related to the reactivity with $O_2$ in the second step of the heme catabolism (see Scheme 1). Bonnett et al. previously proposed that **2a** itself, which means iron(III) *meso*-hydroxyporphyrin, is an intermediate in verdoheme formation, where $O_2$ directly adds to **2a**. However, this reaction could not be allowed because of the spin restriction between the porphyrin and $O_2$.

The molecular orbital (MO) calculation indicated that *meso*-hydroxyporphyrin has two nearly degenerated HOMOs, $a_2$ and $b_2$. When the $\pi$-neutral radical is generated, one electron is ejected from either the $a_2$ or the $b_2$ orbital and transferred to the iron. Because the MO calculation also showed that a large spin density exists at the pyrrole $\alpha$-carbon adjacent to the heme hydroxyl group in its neutral radical state, irrespective of $A_2$ and $B_2$, $O_2$ can directly add to this position in the $\pi$-radical state, followed by the cleavage at the *meso* position. Therefore, it is likely to conclude that **2c** in the mixed state is a key intermediate in the heme breakdown.

Our present results for the model compounds can be extrapolated to a biologically relevant system, i.e., the heme oxygenase system. Recent studies show that the heme in heme oxygenase binds to the protein moiety through the N-ligand most probably from the histidyl imidazole, yielding a five-coordinated heme iron.[29,30] So it seems reasonable to suggest that **2a** in heme oxygenase is in a five-coordination. Our present study implies that coordination of the axial ligand modulates the population of iron(III) *meso*-oxyporphyrin (**2b**) and the neutral radical state (**2c**) through control of the redox property of the iron. In general, the redox potential of the heme iron is more positive in the five-coordination high-spin state than in the six-coordination low-spin state; therefore, assuming that the *meso* hydroxyl group is deprotonated in the enzyme, it can be

(24) Barley, M.; Becker, J. Y.; Domazetis, G.; Dolphin, D.; James, B. R. *J. Chem. Soc., Chem. Commun.* **1981**, 982−983.
(25) (a) Traylor, T. G.; Nolan, K. B.; Hildreth, R.; Evans, T. A.; Srivatsa, G. S. *J. Am. Chem. Soc.* **1983**, *105*, 6149−6151. (b) Sawyer, D. T.; Traylor, D. T. *Inorg. Chem.* **1985**, *24*, 4733−4735.
(26) Lexa, D.; Momenteau, M.; Mispelter, J. *Biochim. Biophys. Acta* **1974**, *338*, 151−163.
(27) Sano, S.; Sugiura, Y.; Maeda, Y.; Ogawa, S.; Morishima, I. *J. Am. Chem. Soc.* **1981**, *103*, 2888−2889.
(28) Safo, M. K.; Gupta, G. P.; Watson, C. T.; Simonis, U.; Walker, F. A.; Scheidt, W. R. *J. Am. Chem. Soc.* **1992**, *114*, 7066−7075.
(29) Takahashi, S.; Wang, J.; Rosseau, D. L.; Ishikawa, K.; Yoshida, T.; Host, J. R.; Ikeda-Saito, M. *J. Biol. Chem.* **1994**, *269*, 1010−1014.
(30) Takahashi, S.; Wang, J.; Rosseau, D. L.; Ishikawa, K.; Yoshida, T.; Takeuchi, N.; Ikeda-Saito, M. *Biochemistry* **1994**, *33*, 5531−5538.

suggested that intramolecular electron transfer from the porphyrin moiety to the iron is favorable. Thus the porphyrin $\pi$-radical state is predominant in the heme oxygenase system. Eventually, **2a** in heme oxygenase is highly reactive toward $O_2$, followed by formation of verdoheme.

In conclusion, we found that **2a** in pyridine is in the resonance hybrid of iron(III) (**2b**) and the porphyrin $\pi$-neutral radical (**2c**) states and that their population is modulated by the ligand basicity. Because **2c** is highly reactive toward $O_2$, the formation of **2c** is essential for the following reaction with $O_2$ to yield verdoheme and to cleave the porphyrin ring. Our present results support Schemes 1 and 2 in the heme degradation system.

**Acknowledgment.** We are grateful to Dr. H Ohya-Nishiguchi and Mr. K. Ichimori for the molecular orbital calculation of **2c**. We also thank Professor F. Anbe for Mössbauer measurements of **2c**.

IC940807Q